The dynamics of water evaporation from partially solvated Cytochrome *c* in the gas phase

Michal Z. Steinberg[(a)], Kathrin Breuker[(b)], Ron Elber[(c)] and R. Benny Gerber[(a),(d)]

(a)Department of Physical Chemistry and the Fritz Haber Research Center, The Hebrew University, Jerusalem 91904, Israel

(b) Institute of Organic Chemistry and Center for Molecular Biosciences Innsbruck (CMBI), Innsbruck University, Innrain 52a, 6020 Innsbruck, Austria

(c)Department of Computer Science, Cornell University, Ithaca, NY 14850, USA

(d) Department of Chemistry, University of California, Irvine CA 92697, USA

Abstract

The study of evaporation of water from biological macromolecules is important for the understanding of electrospray mass spectrometry experiments. In electrospray ionization (ESI), electrically charged nanoscale droplets are formed from solutions of, for example, proteins. Then evaporation of the solvent leads to dry protein ions that can be analyzed in the mass spectrometer. In this work the dynamics of water evaporation from native Cytochrome *c* covered by a monolayer of water is studied by Molecular Dynamics (MD) simulations at constant energy. A model of the initial conditions of the process is introduced. The temperature of the protein drops by about 100ºK during the 400 picoseconds of the simulations. This sharp drop in temperature causes the water evaporation rate to decrease by about an order of magnitude, leaving the protein with 50% to 90% of the original water molecules, depending on the initial temperature of the simulation. The structural changes of the protein upon desolvation were considered through calculations of the radius of gyration and the Root Mean Square (RMS) of the protein. A variation of 0.4 Å in the radius of gyration, together with a RMS value of less than 3 Å indicates only minor changes in the overall shape of the protein structure. The water coordination number of the solvation shell is much smaller than that for bulk water. The mobility of water is high at the beginning of the simulations and drops as the simulation progresses and the temperature decreases. Incomplete desolvation of protein ions was also observed in recent experiments.

1. Introduction

A detailed atomic-level description of the mechanisms by which water molecules affect proteins is important for the understanding of protein structure and stability. Because detailed protein structures in the gas phase are not yet available, the most promising approach for studying the effect of hydration on protein structure and stability is to start with the known structure in aqueous solution, and follow possible changes upon evaporation of the water. This can be done in computational studies as reported here, or in electrospray ionization (ESI)[1,2] experiments. Two models for the formation of solvent-free ions in ESI have been suggested: the ion evaporation model (IEM)[3] , and the charge residue model (CRM)[4,5]. In both models, the electrically charged droplets from ESI first undergo multiple fissions to form very small droplets[6-9]. The IEM suggests that partially solvated ions are ejected from small droplets (~10 nm radius), whereas the CRM proposes solvent evaporation from even smaller droplets (<3 nm radius)[10]. However, little is known to date about the final stages of ion desolvation in ESI. Computational studies on the evaporation of water from biological macromolecules could substantially increase our understanding of the desolvation process in ESI.

ESI of biomolecules from non-denaturing solutions ("native ESI") is believed to proceed via CRM[11-13], suggesting that their native structure is preserved at least until the very last stages of ion desolvation. However, native electron capture dissociation (NECD)[14] experiments on equine Cytochrome *c* revealed different degrees of local stability for different regions of the protein in the transition from solution to gas phase. This order of regional stability was essentially the reverse of the order in

solution, which was attributed to the loss of hydrophobic bonding and the strengthening of electrostatic interactions in the absence of bulk water[15]. While the reversed order of local stability necessitates unfolding of the native Cytochrome *c* structure in the gas phase, experiments have not provided an exact time scale for this process. Ion mobility studies on the +7 to +10 ions of Cytochrome *c* stored in an ion trap at 300ºK showed unfolding transitions on a millisecond timescale but with induction periods of ~30 ms[16]. A possible reason for these induction periods was attributed to ion cooling below the ambient temperature and conformational freezing as a result of solvent evaporation during the ESI process[16,17]. Partially hydrated peptides[18,19] and proteins[20] in electrospray experiments have also been reported. Liquid water beam desorption mass spectrometry is another experimental technique where conformational freezing is indicated. This technique has recently been used by Abel *et al* for the study of macrobiomolecules in the gas phase[21]. The issues of conformational freezing and partial hydration are addressed in the present work by computational studies on equine Cytochrome *c*.

Our understanding of electrospray experiments of native biological systems could greatly benefit from theoretical modeling[22-26]. Since biomolecular systems are large and water molecules are small, a combination of efficient methodology that retains the atomically detailed description of the system is desired. This is the Molecular Dynamics (MD)[27,28] approach. Mao, Ratner and Jarrold[29-31] have studied by MD the effect of ion net charge on the compactness[29], stability[31] and hydration[30] of unsolvated Cytochrome *c* ions, and found qualitative agreement with results from ion mobility experiments which showed that the lower charge states are geometrically more compact and stable than the higher charge states, and that the compact ions absorb

more water molecules[32,33]. The +3 to +8 ions exhibited collision cross section values close to that predicted for the native Cytochrome *c* structure[32,34,35]. In a similar approach using MD calculations and collision cross sections from ion mobility experiments, Bowers and coworkers concluded that G-quadruplex structures can be conserved in a solvent-free environment[36]. Orozco[37,38] *et al* have studied complexes of DNA with minor groove binders in the gas phase by MD. They found that solvent evaporation does not change the gross structural, energetic and dynamic features of the DNA, and does not produce dissociation of the drug from the DNA. The study of completely desolvated proteins in the gas phase by MD has recently been reviewed by Arteca, Reimann, and Tapia[39].

Protein Hydration was studied theoretically in the past[40]. Previous studies of hydration levels of Myoglobin[41,42] by MD suggest that a moderate water coverage of ~350 water molecules for Myoglobin is needed in order to conserve native structural properties of the protein. Merzel and Smith[43-45] studied by MD the density of water molecules that surround a protein. They found that the density of the first water layer around a protein is higher than the density of bulk water.

Evaporation of water molecules from a surface of a protein involves breaking of noncovalent bonds between water and protein atoms as well as between different water atoms. Thus the evaporation process not only models the final stages of ESI, but also gives detailed insight into the interaction of a protein with its environment. We also expect to improve our understanding of the local noncovalent forces at different regions of the protein surface. Valuable information on protein interaction with water molecules has been also obtained from experiments in solution[46-48].

In the present investigation the evaporation of water from Cytochrome *c* is studied computationally. Molecular Dynamics simulations of Cytochrome *c* covered with a monolayer of water were carried out in order to answer the following questions. How do the water molecules arrange around the protein? How mobile are the water molecules? How is the kinetic energy partitioned between the protein and the water molecules during the evaporation process? What happens to the temperature of the protein during the desolvation process?

Equine Cytochrome *c* is an electron transfer protein composed of 104 amino acids and a covalently attached heme group. Cytochrome *c* is a useful model for water evaporation studies as it has been extensively studied in solution[49] and in the gas phase[50].

Section 2 below focuses on computational methods and on the initial state of the protein and its solvation. Temperature, dynamics and structural properties of the system are reported in section 3. Concluding remarks are the topic of Section 4.

2. System and Methods

2.1. The Force Field

The MOIL suite of programs[51] was used in the atomistic detailed simulations. The MOIL force field is based on AMBER and OPLS force fields. In MOIL only polar hydrogen atoms are treated explicitly in the dynamics. Covalently bound hydrogen

atoms such as in the CH_n groups are described as part of an "extended atom". Water molecules were explicitly represented by the TIP3P model[52]. TIP3P water model is non-polarizable and was originally parametrized for bulk water. It might therefore not be ideal for studies of this type. More advanced model such as TIP5P[53] might be better suited for the study of evaporation phenomena. We assume that for the semi-quantitative objective of this study, polarization effects are unlikely to affect the main findings.

2.2. Model of the initial state

The model adopted here corresponds to a protein covered with a thin layer of water, initially taken to be at a selected temperature. This model droplet is not coupled to a thermal bath. Evaporation events are therefore necessarily at the expense of internal energy of the system. Different initial temperatures were used in order to explore the effect of internal energy on water evaporation.

All simulations in this work are based on the NMR structure of native oxidized (Fe^{III}) horse heart Cytochrome *c* which was solved by Banci *et al*[54] (protein data bank entry 1AKK). The native structure was covered with 182 water molecules to form an approximate monolayer of water by two different procedures. In the first procedure the protein was placed in a water box of 30Å×30Å×30Å with 201 water molecules. The system was then partially relaxed by a 10 psec simulation at 10°C with no geometric constraints and at constant energy. After the initial relaxation all water molecules that escaped the surface of the protein were removed. The resulting initial water distribution is non-uniform as the water molecules aggregate near the charges

on the surface and leave patches of non charged areas uncovered. In the second procedure the protein was placed in a water box and without any relaxation all water molecules more than 4.65 Å away from any protein atom were removed. The 4.65 Å cutoff was chosen so 182 water molecules would remain on the protein surface to give the same amount of water molecules as in the first procedure. The initial structure formed by this method is characterized by a more uniform water arrangement around the protein but in a less stable structure. These two initial structures are shown in Figure 1.

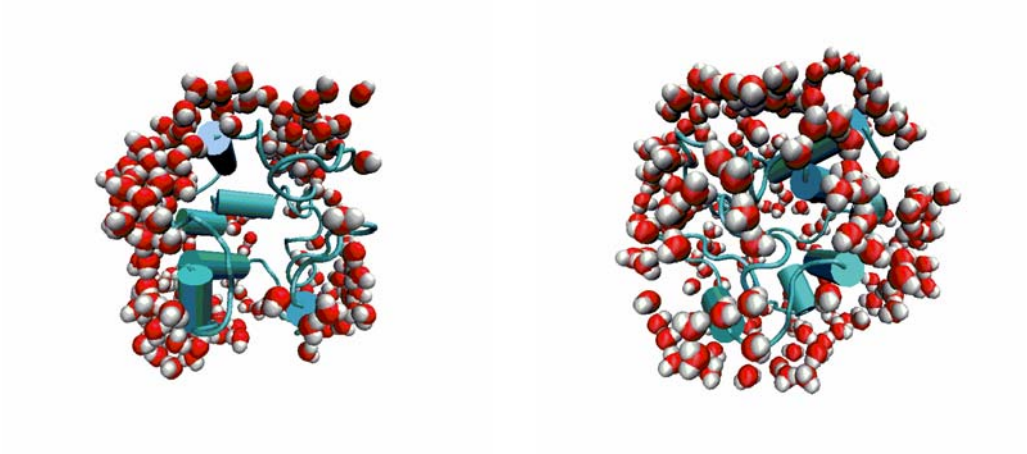

Figure 1: Native Cytochrome *c* (shown as cartoons without the heme group) surrounded by 182 water molecules (shown by red balls for the oxygen and white balls for the hydrogens). Left: Water arrangement after relaxation. Right: Water arrangement without relaxation.

In the relaxed initial conformation (Figure 1,left) the hydration shell of 182 water molecules is not a uniform monolayer but a patchwork of water clusters, covering primarily the charged groups such as the protonated lysine and arginine residues and the deprotonated aspartic acid and glutamic acid residues while leaving other areas of

the surface uncovered. The water molecules are arranged such that their density is higher on the exposed areas of the alpha helices and lower in the loop regions.

The two structures in Figure 1 were used as starting structures for the MD simulations. The different initial kinetic energies used in the calculations correspond to temperatures ranging from 60°C to 170°C. Charge sites were assigned according to calculated pK_a values of the ionizable residues in native (Fe^{III}) Cytochrome *c*[55] at pH 5 (for details, see reference[56]). Briefly, all Aspartic and Glutamic acid residues, both heme propionates and the C-terminus are deprotonated, all Lysine and Arginine residues are protonated, and the Histidine residues are uncharged to give a net charge of +6.

2.3 Dynamics

The evaporation of water molecules from the surface of Cytochrome *c* was studied by Molecular Dynamics simulations. All simulations were performed with MOIL, which is a modeling package for simulations of biological molecules. The simulations were done in vacuum conditions at constant energy. Two different options of the SHAKE algorithm[57] in MOIL were used. The light SHAKE freezes only vibrations of bonds that contain hydrogen atoms. The regular SHAKE freezes fast vibrations of all bonds. All the water molecules are treated as rigid objects.

Ten different trajectories of 400 picoseconds were simulated with different initial conditions. Seven trajectories were computed for the relaxed water conformation with

initial temperatures of 354ºK, 379ºK, 380ºK, 399ºK, 421ºK, 447ºK and 470ºK. Light SHAKE was used for the higher temperatures and regular SHAKE was used for the lower temperatures where it was found to better conserve the energy. The time step in all the simulations was 0.2 femtoseconds. This is significantly lower than the 1 femtosecond step used in most MD simulations but was necessary to maintain a high level of energy conservation. No cutoff distance for non-bonded interactions was used.

The quantitative properties of the evaporation process computed in this work include the temperature of the system, the temperature of the protein, the evaporation rate, the water diffusion coefficients, the RMS of the protein and the radius of gyration of the protein.

3. Results

3.1. Protein temperature as a function of time

a. The temperature of the protein is computed based on the kinetic energy of all atoms in the protein. The system is assumed to be in equilibrium, though strictly speaking it is not. We assume that after a short time of a few hundred femtoseconds the system reaches a partial equilibrium state with respect to the kinetic energy. The temperature is therefore computed by:

$$T = \frac{2}{3} * \frac{\text{Average Kinetic Energy}}{\text{K}_{\text{Boltzmann}}} \qquad (1)$$

In Figure 2 we show the drop in protein temperature during the evaporation process. The cooling of the system upon evaporation of water molecules is due to the fact that the breaking of water – protein non covalent bonds occurs at the expense of kinetic energy of the system. In addition, the evaporating water molecules carry kinetic energy with them which also decreases the temperature of the protein. This MD result is in qualitative agreement with "native" protein electrospray experiments by Loo[20] (Figure 3). The mass spectra provide evidence that in the absence of sufficient external heating, the protein remains partially hydrated in the electrospray experiment process. In the top panel of Figure 3 the temperature of the metal capillary through which the protein ions enter the mass spectrometer was about 100°C. The broad shape of the peaks was attributed to water molecules that remained attached to the protein. For the bottom spectrum in Figure 3, a temperature of 200°C was applied. The resulting sharp peaks in this case indicate a much higher degree of protein desolvation. Preliminary results from MD simulations at constant temperature conditions (not shown here) show that additional heating of the protein/water system at room temperature can lead to full desolvation of the protein. A full report of this is in preparation.

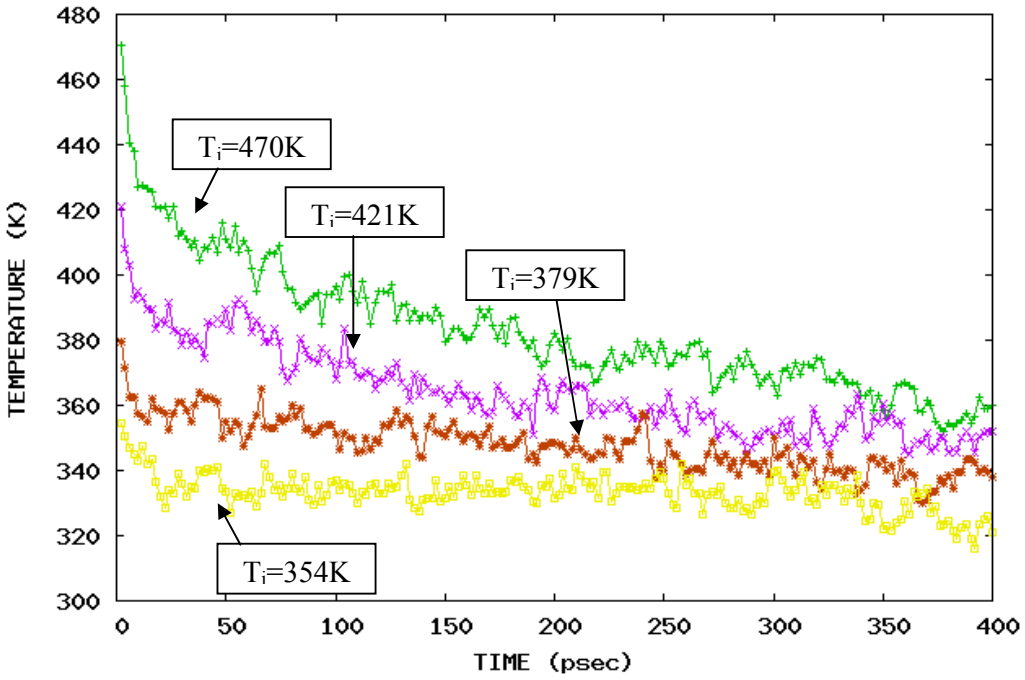

Figure 2: Protein temperature *vs*. time for different initial temperatures, T_i

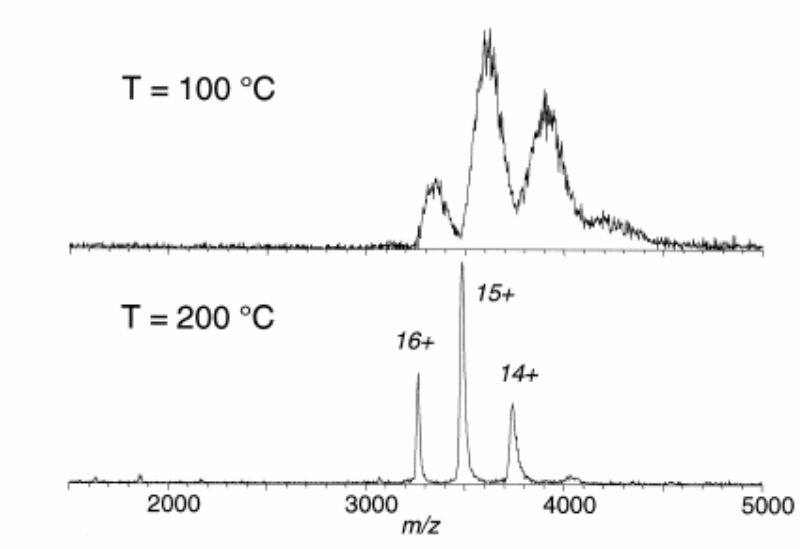

Figure 3: "Native" electrospray mass spectra of streptavidin (from reference [*J.A. Loo/International Journal of Mass Spectrometry 200 (2000) 175–186*], reprinted with

permission). The protein solution is electrosprayed into a metal capillary that can be heated to assist desolvation. With a capillary temperature of 100°C (top spectrum), desolvation is incomplete as evidenced by the broad peaks in the *m/z* spectrum. Increasing the temperature to 200°C (bottom spectrum) greatly improves the desolvation process, and the resulting peaks are sharpened.

3.2. Water evaporation rate

The evaporation rate as a function of time is plotted in Figures 4 and 5 for different initial temperatures. In Figure 4 the evaporation rate is plotted for Cytochrome *c* covered with 182 water molecules that were relaxed around the surface of the protein by a short MD. In this case the water molecules were located on the surface at energetically favorable positions near charge sites and were more stable with respect to detachment from the surface.

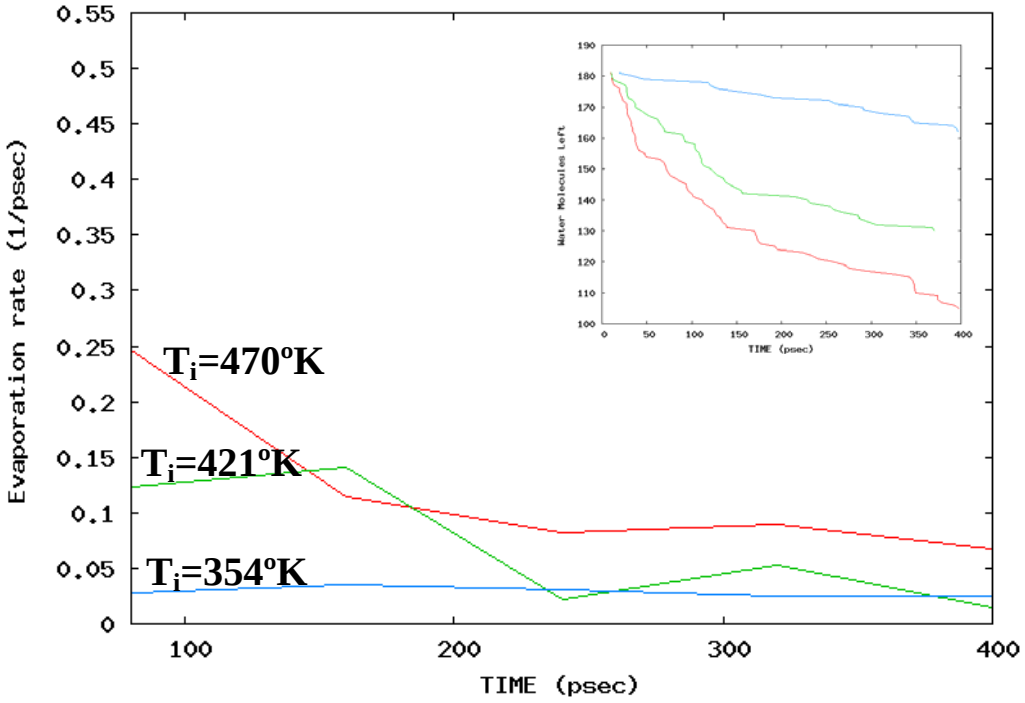

Figure 4: Water evaporation rate *vs*. time for different initial temperatures, T_i, for native Cytochrome *c* covered with 182 water molecules that were relaxed around the protein. The figure at the top right shows the number of water molecules left on the protein surface *vs*. time for different initial temperatures, T_i.

In Figure 5 the evaporation rate is plotted for Cytochrome *c* covered with 182 water molecules that were more uniformly arranged on the protein surface. In this case the water molecules were not relaxed to energetically stable sites on the surface of the protein and were therefore less attached to the surface. It is clear from the two graphs that the evaporation rates for the unrelaxed water molecules are higher than the evaporation rate for the relaxed water molecules. In both cases the evaporation rate increases for higher initial temperatures, though after an initial "ballistic" period all rates become similar rather quickly. Limited statistics forbids more precise conclusions.

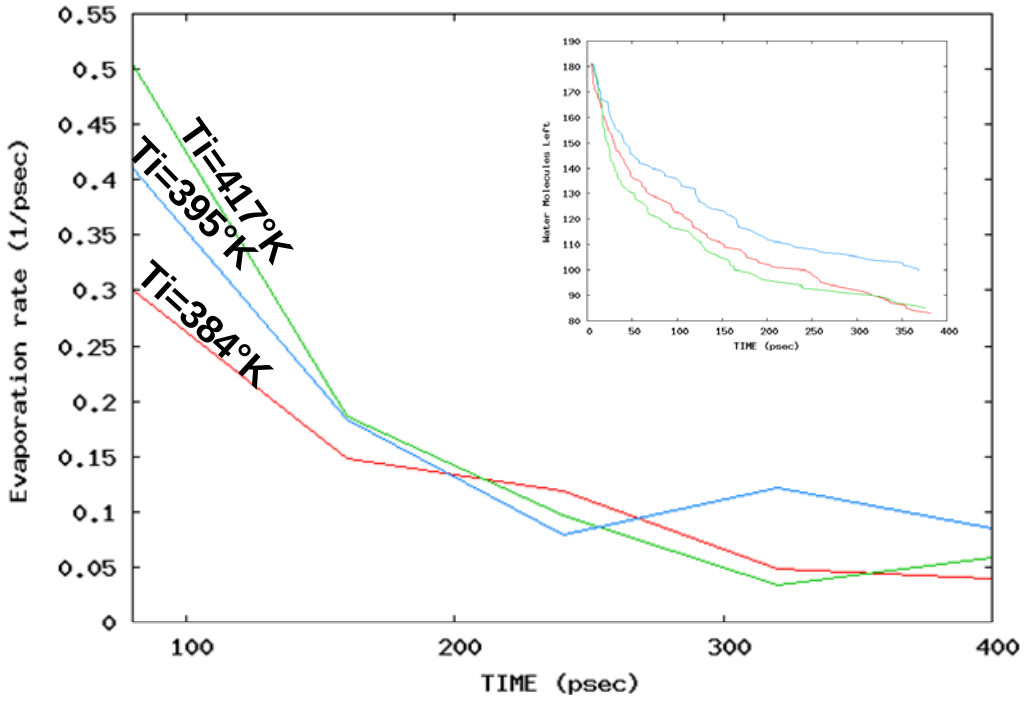

Figure 5: Water evaporation rate as a function of time for different initial temperatures, T_i, for native Cytochrome *c* covered with 182 water molecules that were uniformly arranged around the protein. The figure at the top right shows the number of water molecules left on the protein surface *vs*. time for different initial temperatures, T_i.

Because the temperature of the system drops during the evaporation process, the evaporation rate decreases until it becomes so small that the water molecules are frozen on the surface of the protein on the time scale of the simulation. The amount of water molecules left on the surface was found to be smallest for the hottest trajectory with non relaxed water conformation for which only 87 out of the initial 182 water molecules were left attached. The number of water molecules that remained on the surface is largest for the coldest trajectory (T_i=354ºK) with the relaxed water conformation. A total of 163 out of the 182 water molecules originally covering the

surface of the protein remained attached in this case. This provides an indication of how different the water loss can be for different initial structure and energy.

3.3. Water coordination numbers

The coordination number of a water molecule is defined as the number of neighboring water molecules with an oxygen-oxygen distance of 3.1Å or less. The water coordination number was approximately the same for all trajectories reported here. Figures 6 and 7 illustrate the difference between surface and bulk water. The water coordination number was calculated to have a maximum probability of one for water on the protein surface, and a maximum probability of four for bulk water. This lower coordination number on the surface of the protein is attributed to water arrangement around the protein with characteristics of a two dimensional structure rather than the three dimensional structure of bulk water.

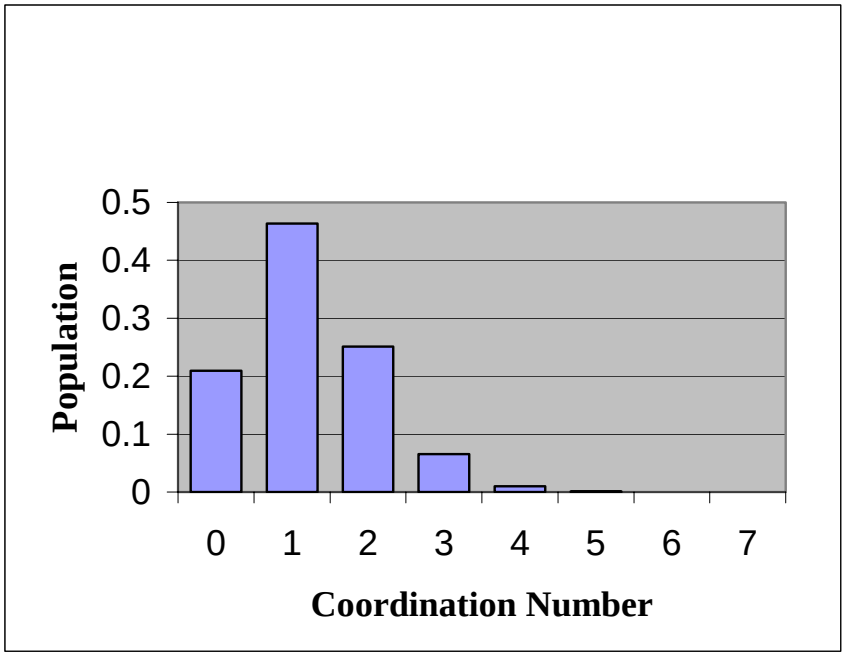

Figure 6: Histogram for coordination of water on the surface of Cytochrome *c* from an average over all times of the trajectory.

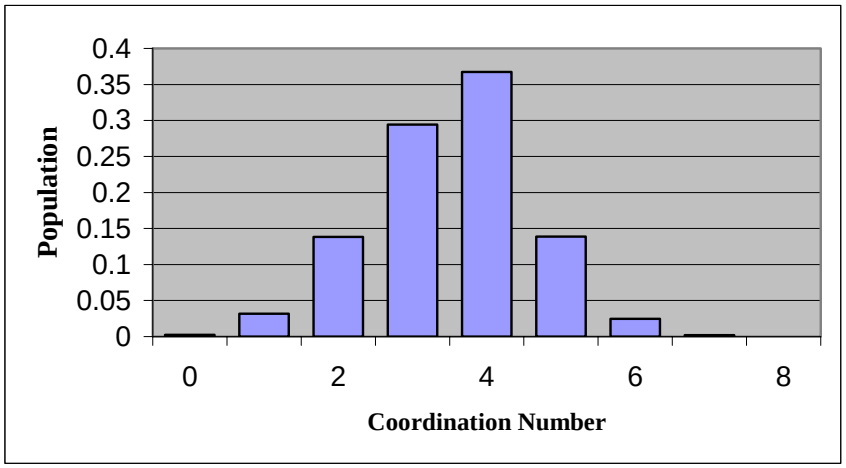

Figure 7: Histogram for coordination of bulk water calculated with the "pure water box" of the Moil package.

3.4. Lifetime of pair of water molecules

A water pair is defined when two water molecules are 4Å apart or closer. The histogram of the number of water pairs, averaged over all the ten trajectories, as a function of the lifetime is plotted in Figure 8. The lifetime of a water – water pair is of no more than a few tens of picoseconds, indicating rapid movements of the water molecules on the protein surface.

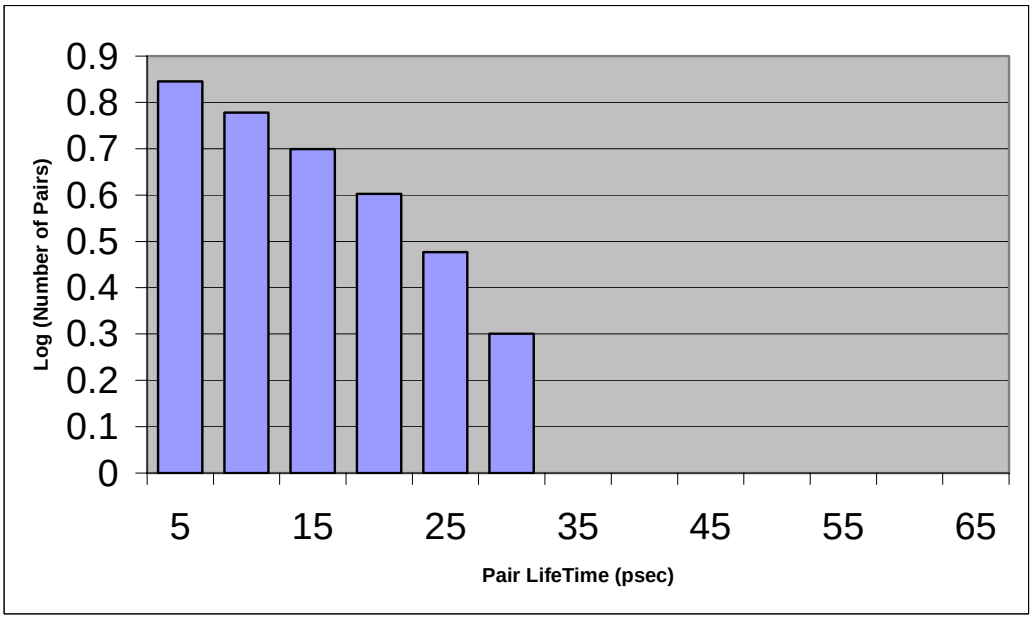

Figure 8: The log of the number of water pairs as a function of lifetime. Note that the relaxation deviates from exponential behavior.

3.5. Water Diffusion Coefficient

The Diffusion Coefficient was calculated from the mean square displacement function[58]

$$6Dt = \left\langle \left[\mathrm{r}(\tau + t) - \mathrm{r}(\tau) \right]^2 \right\rangle \qquad (2)$$

Where t is the time offset that was taken to be 1psec and τ is a specific time, <…> denotes an average over time origins τ and over a species of molecules of interest, and r(τ) is the position of the molecule at time τ.

The diffusion coefficient depends on the temperature. As a result of the drop in temperature during the evaporation process the diffusion coefficient drops with time. We therefore calculated the diffusion coefficient at time intervals of 10 picoseconds and plotted it as a function of temperature for different trajectories in Figure 9. The dependence of the diffusion coefficient on the temperature was found to be the same for trajectories of the same initial structure regardless of the initial temperature. The

two trajectories of Figure 9 are therefore examples of the two different initial structures.

It is clear from Figure 9 that the diffusion coefficient does not depend only on temperature but also on the initial state of the system. The trajectories with the non-relaxed water conformation have higher diffusion coefficients than the trajectories with the relaxed water conformation. The reason for the latter is that the water in the non relaxed water conformation are less attached to the protein and are therefore more free to move around the surface of the protein.

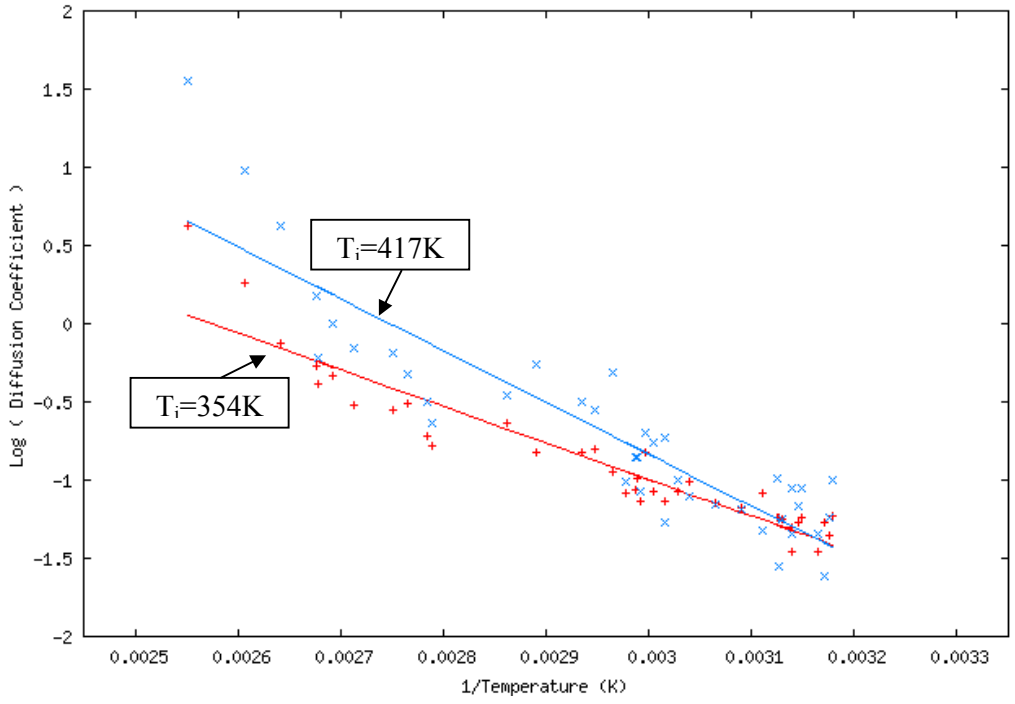

Figure 9: The diffusion coefficient (in m^2/sec), on a logarithmic scale, *vs*. the inverse of the temperature, for different initial temperatures, T_i. The blue line and dots correspond to a trajectory that was started from a non relaxed water conformation and therefore shows higher diffusion rates than the one calculated for the red data which corresponds to a trajectory calculated from a relaxed water conformation.

The regular diffusion coefficient is defined for equilibrium conditions which do not apply here. Yet the system does reach a quasi steady state after a few hundred femtoseconds. The activation energy for diffusion can be calculated from equation (3) and was found to range from 4.7 ± 0.3 kcal/mol to 7.3 ± 0.3 kcal/mol depending on the initial conditions. The highest effect of the initial conditions is at the beginning of the trajectory before the system reaches quasi equilibrium, when the fit to a straight line is poorest.

$$D = D_0 e^{-\frac{E_a}{K_b T}} \Rightarrow \log(D) = \log(D_0) - \frac{E_a}{K_b T} \qquad (3)$$

Where, D is the diffusion coefficient, D_0 is the Diffusion constant at T → infinite temperature, E_a is the activation energy K_b is the Boltzmann constant and T is the temperature.

Since the surface of the protein is not uniform, with regards to electrostatic forces and steric effects, there is a distribution of barriers for diffusion. This may lead to a distribution of diffusion coefficients corresponding to different regions of the surface.

3.6. Structural properties of the protein

The structural properties of the protein were analyzed by two means, the Radius of gyration of the protein and the root mean square (RMS) of the protein.

Radius of gyration

The Radius of Gyration was calculated from:

$$Rg = \sqrt{\frac{\sum m_i r_i^2}{\sum m_i}} \tag{4}$$

Where m_i is the mass of atom i and r_i is the distance of atom i from the center of mass. Water molecules were not taken into account in these calculations.

The Radius of gyration was roughly constant throughout the simulations with an average value of 12.64 Å for which the standard deviation was 0.4 Å.

RMS of the protein

The conformational changes of the protein are described by the all atom Root Mean Square (RMS) deviation from the initial structure:

$$RMS_i = \sqrt{\frac{1}{N_D}\sum_{\alpha=1}^{N_D}\left[r_\alpha(t_i) - r_\alpha(t_0)\right]^2} \tag{5}$$

Where $r_\alpha(t_i)$ and $r_\alpha(t_0)$ are the coordinate sets of the i'th structure and the initial structure and N_D is the number of atoms in the protein.

As can be seen from Figure 10, the change in the protein's RMS hardly exceeds 3Å which means that the structural changes are relatively small, and the overall shape of the protein is maintained during the simulations.

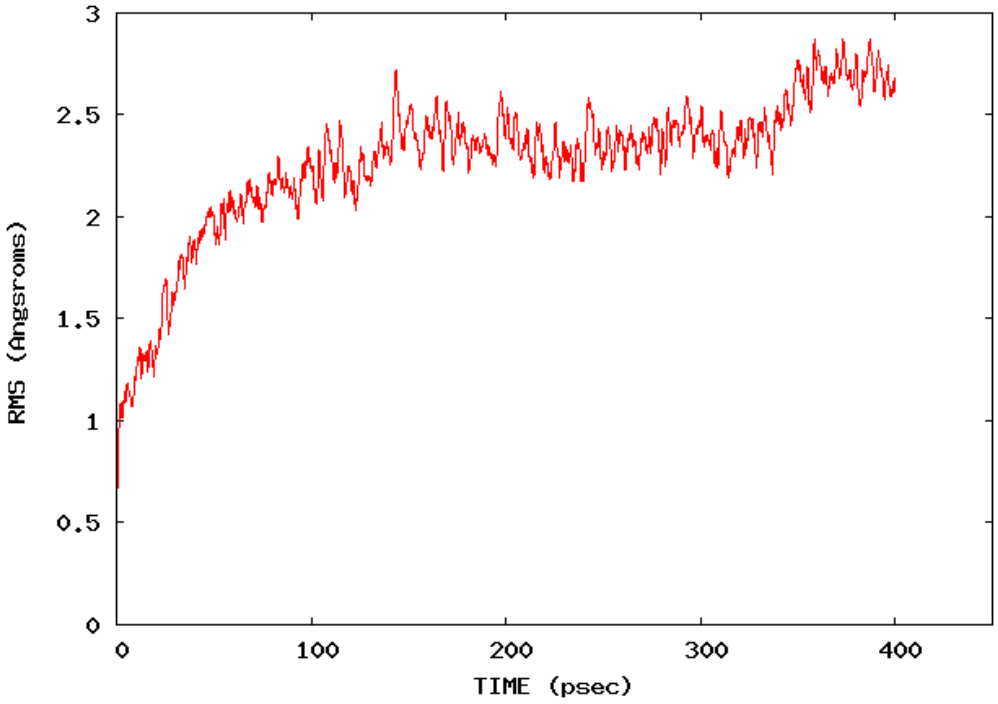

Figure 10: The all atom RMS of the protein for the trajectory started at 439°K

Comparison between the initial structure of the protein and the final structure can be seen in figure 11. It can be visualized from the figure that there are barely any changes in the backbone structure of the protein.

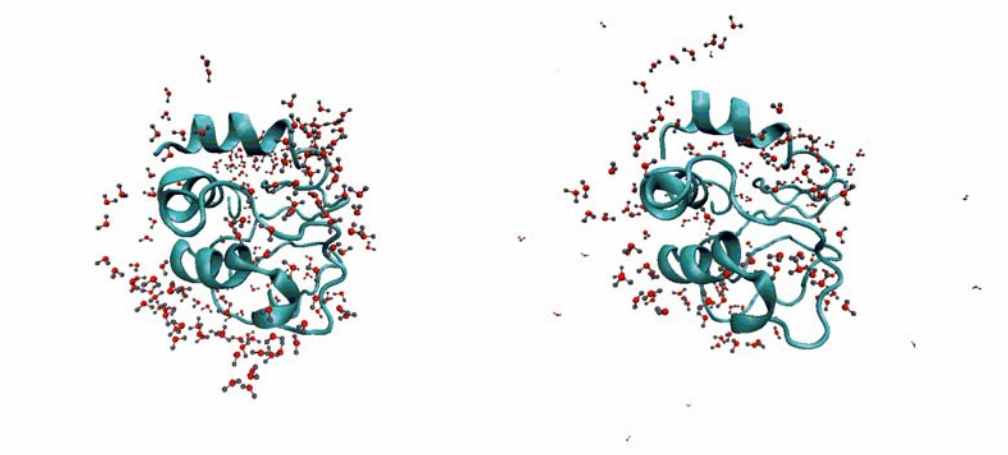

Figure 11: Native Cytochrome *c* (shown as cartoons without the heme group) surrounded by 182 water molecules (shown by red balls for the oxygen and gray balls for the hydrogens). Left: Initial structure. Right: Final structure, after simulation of 400 psec.

The conclusion from the radius of gyration, RMS analysis and visualization of the structure is that under the condition of energy conservation, the overall structural changes of the protein upon desolvation are small.

Lysine side chains are very long and flexible. They are mostly found on the surface of the protein due to the charge at the end of their long "tail" that is stabilized by solvation by water. These side chains were found to move and stretch more than other parts of the protein. This property is described in more details in the next section.

3.8. **Structural changes with time during the evaporation dynamics**

Different kinds of evaporation mechanisms are evident from the simulations. Most of the time the evaporation process involves a single water molecule but in some rare events evaporation of a dimer occurs. Figure 11 below shows snapshots of the system at different times of the simulation. At the beginning the system is dense as the water molecules are close to the surface of the protein. As the simulation proceeds the water molecules that are not yet evaporated are positioned further away from the surface of the protein. The whole system seems to expand. At the end of the simulation the remaining water molecules are mostly located around the charge sites of the lysine side chains. The lysine side chains are long and flexible, and in solution their charged ends tend to point away from the protein surface. Water molecules aggregate near the charged end of the lysines and stabilize the charge.

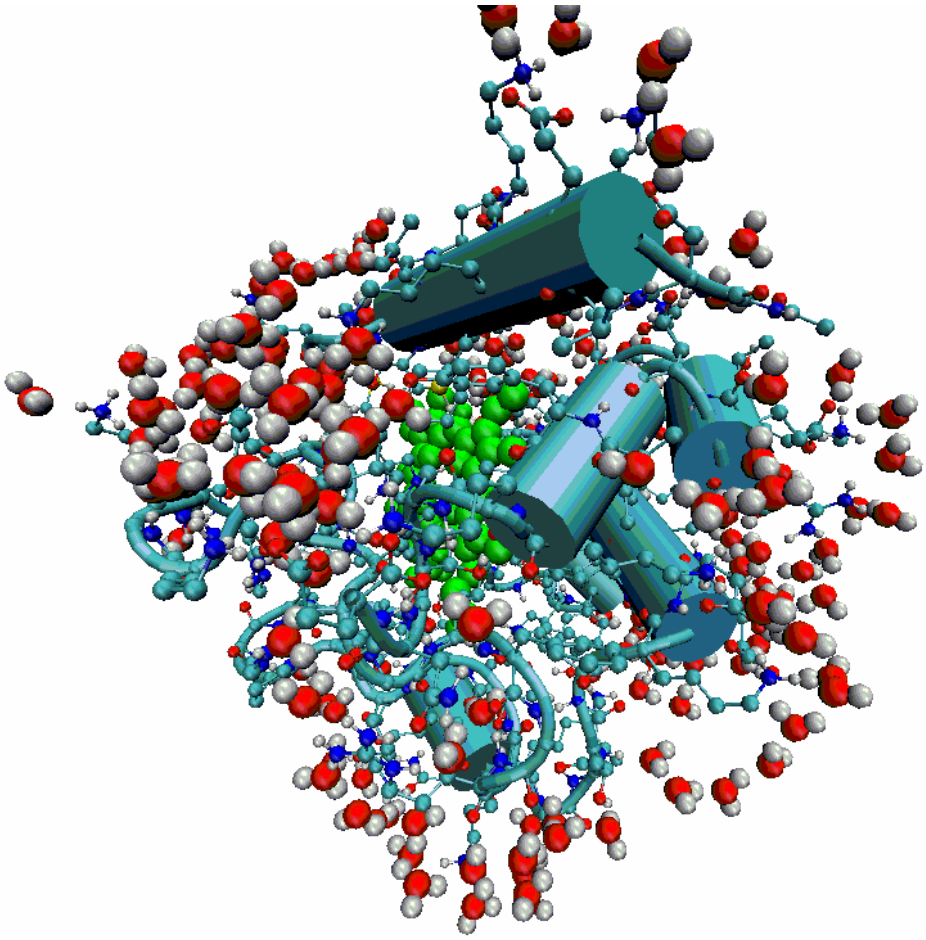

(a)

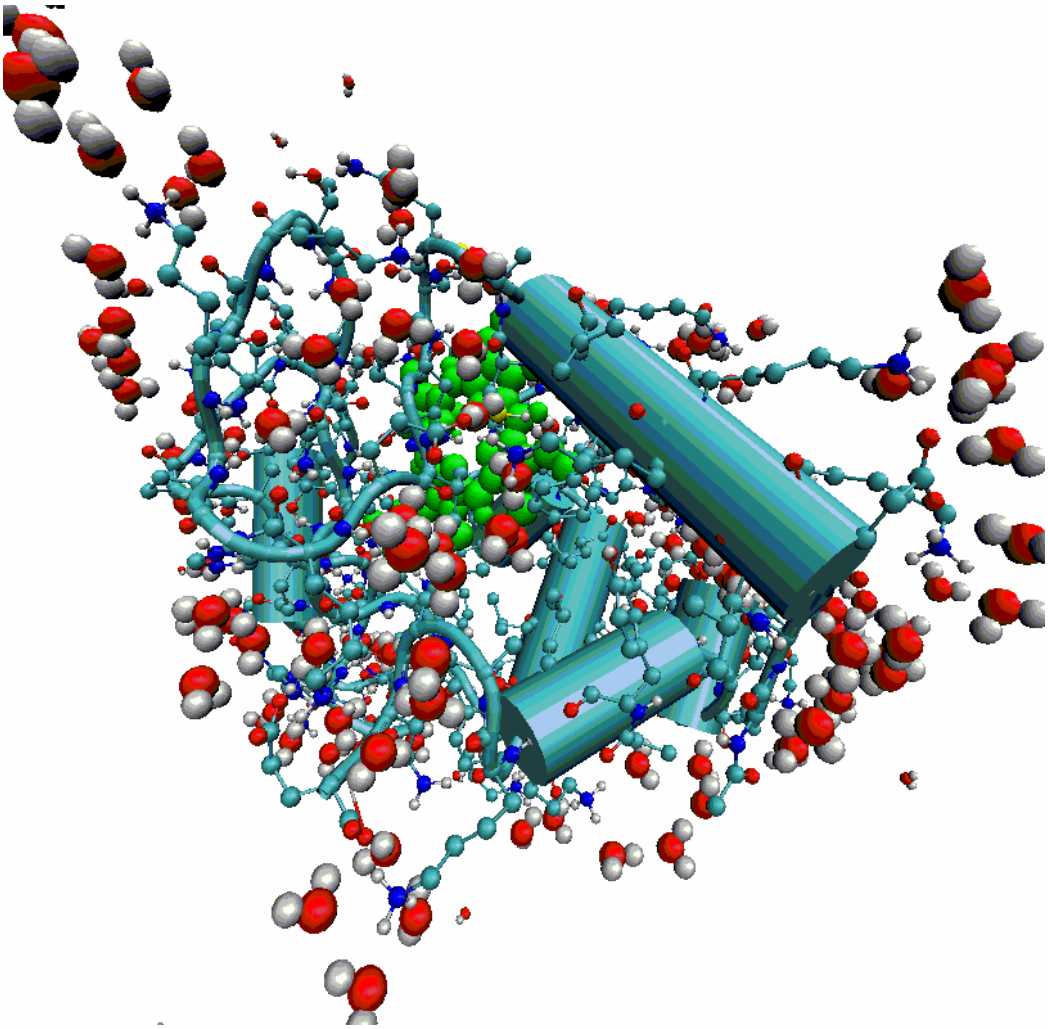

(b)

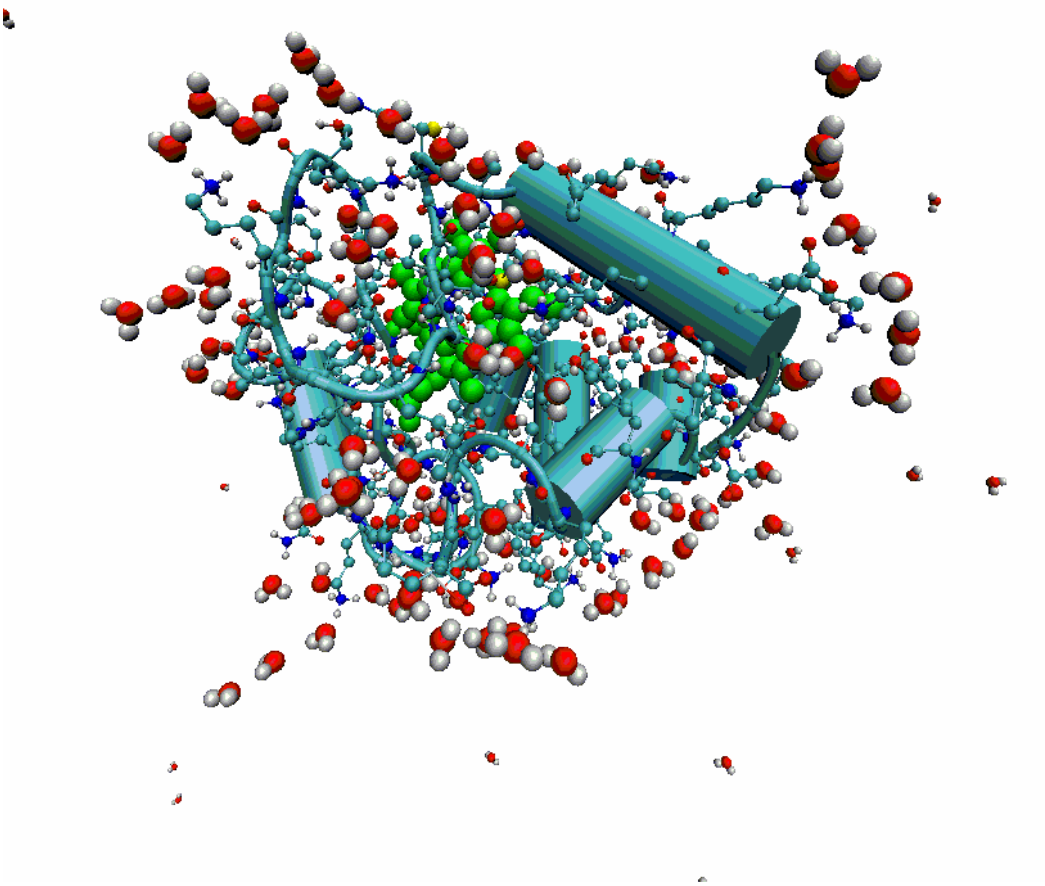

(c)

Figure 12: Snapshots of the system at different times of the simulation. Native Cytochrome *c* (shown as cartoons) surrounded by 182 water molecules (shown by red balls for the oxygen and white balls for the hydrogens) with the heme group (shown in green) and the lysine side chains (shown in balls and stick format). (a) The initial state. The water molecules here are very dense on the surface of the protein. (b) After 200 picoseconds. The arrangement of the water molecules expands to longer distances from the surface of the protein. (c) After 400 picoseconds. Most of the remaining

water molecules are attached to the $-NH_3^+$ groups of the Lysine sidechains which point away from the surface of the protein.

4. Concluding remarks

Mass spectrometric methods and in particular electrospray ionization techniques have emerged in recent years as indispensable tools for the study of biological macromolecules in the gas phase. So far only limited understanding is available of the mechanisms involved in ESI. In the present paper an attempt was made to deal with an important aspect of ESI, namely the evaporation of water from the surface of the protein following the formation of nano droplets. The molecular dynamics simulations carried out here show several characteristics of this evaporation process. First when starting with a monolayer of hydration water and realistic initial temperatures, only a limited fraction of the water (10-50%) evaporates under energy conservation conditions. The early loss of water molecules leads to rapid cooling on the order of up to ~100ºK during the first 100 picoseconds, after which the remaining water molecules are "frozen" on the surface. It also seems that there are no major structural changes of the protein during the evaporation stage. Another observation is that the remaining sub monolayer involves water molecules of low coordination. Our results are relevant for the interpretation of electrospray experiments in which only very little energy is provided to facilitate the desolvation process. Heating the protein by infrared radiation and/or collisions with gas molecules during the electrospray process appears to be essential for complete desolvation of proteins. As electrospray ionization is conducted at atmospheric pressure, energy is supplied in all experimental studies, although to different extent. Work in progress studies the evaporation of

water from proteins under constant temperature conditions. We are also pursuing processes on longer timescales and after complete desolvation of the protein. We believe that such molecular dynamics simulations will be helpful in the interpretation of electrospray experiments, as well as for the general understanding of protein structure and stability.

Acknowledgements

The authors thank Fred W. McLafferty for useful discussions. KB acknowledges generous funding from the Austrian FWF and TWF (grants T229, UNI-0404/158). NIH grant 5R01GM059796 to RE is acknowledged for partial support of this work. The research at the Hebrew University was supported under the auspices of the Searree K. and Louis P. Fiedler Chair in Chemistry.

References

(1) Fenn, J. B.; Mann, M.; Meng, C. K.; Wong, S. F.; Whitehouse, C. M. *Science* **1989**, *246*, 64-71.

(2) Smith, R. D.; Loo, J. A.; Edmonds, C. G.; Barinaga, C. J.; Udseth, H. R. *Analytical Chemistry* **1990**, *62*, 882-899.

(3) Iribarne, J. V.; Thomson, B. A. *Journal of Chemical Physics* **1976**, *64*, 2287-2294.

(4) Dole, M.; Mack, L. L.; Hines, R. L. *Journal of Chemical Physics* **1968**, *49*, 2240-&.

(5) Schmelzeisenredeker, G.; Butfering, L.; Rollgen, F. W. *International Journal of Mass Spectrometry and Ion Processes* **1989**, *90*, 139-150.

(6) Tang, K.; Gomez, A. *Physics of Fluids* **1994**, *6*, 2317-2332.

(7) Gomez, A.; Tang, K. Q. *Physics of Fluids* **1994**, *6*, 404-414.

(8) Grimm, R. L.; Beauchamp, J. L. *Analytical Chemistry* **2002**, *74*, 6291-6297.

(9) Smith, J. N.; Flagan, R. C.; Beauchamp, J. L. *Journal of Physical Chemistry A* **2002**, *106*, 9957-9967.

(10) Kebarle, P.; Peschke, M. *Analytica Chimica Acta* **2000**, *406*, 11-35.

(11) de la Mora, J. F. *Analytica Chimica Acta* **2000**, *406*, 93-104.

(12) Felitsyn, N.; Peschke, M.; Kebarle, P. *International Journal of Mass Spectrometry* **2002**, *219*, 39-62.

(13) Verkerk, U. H.; Peschke, M.; Kebarle, P. *Journal of Mass Spectrometry* **2003**, *38*, 618-631.

(14) Breuker, K.; McLafferty, F. W. *Angewandte Chemie-International Edition* **2003**, *42*, 4900-4904.

(15) Breuker, K.; McLafferty, F. W. *Angewandte Chemie-International Edition* **2005**, *44*, 4911-4914.

(16) Badman, E. R.; Hoaglund-Hyzer, C. S.; Clemmer, D. E. *Analytical Chemistry* **2001**, *73*, 6000-6007.

(17) Myung, S.; Badman, E. R.; Lee, Y. J.; Clemmer, D. E. *Journal of Physical Chemistry A* **2002**, *106*, 9976-9982.

(18) Lee, S. W.; Freivogel, P.; Schindler, T.; Beauchamp, J. L. *Journal of the American Chemical Society* **1998**, *120*, 11758-11765.

(19) RodriguezCruz, S. E.; Klassen, J. S.; Williams, E. R. *Journal of the American Society for Mass Spectrometry* **1997**, *8*, 565-568.

(20) Loo, J. A. *International Journal of Mass Spectrometry* **2000**, *200*, 175-186.

(21) Charvat, A.; Bogehold, A.; Abel, B. *Australian Journal of Chemistry* **2006**, *59*, 81-103.

(22) Barran, P. E.; Polfer, N. C.; Campopiano, D. J.; Clarke, D. J.; Langridge-Smith, P. R. R.; Langley, R. J.; Govan, J. R. W.; Maxwell, A.; Dorin, J. R.; Millar, R. P.; Bowers, M. T. *International Journal of Mass Spectrometry* **2005**, *240*, 273-284.

(23) Gerstein, M.; Levitt, M. *Scientific American* **1998**, *279*, 100-105.

(24) Levitt, M. *Chemica Scripta* **1989**, *29A*, 197-203.

(25) Levitt, M. *Abstracts of Papers of the American Chemical Society* **1998**, *216*, U625-U625.

(26) Levitt, M.; Hirshberg, M.; Sharon, R.; Laidig, K. E.; Daggett, V. *Journal of Physical Chemistry B* **1997**, *101*, 5051-5061.

(27) Mccammon, J. A.; Gelin, B. R.; Karplus, M. *Nature* **1977**, *267*, 585-590.

(28) Karplus, M.; McCammon, J. A. *Nature Structural Biology* **2002**, *9*, 646-652.

(29) Mao, Y.; Ratner, M. A.; Jarrold, M. F. *Journal of Physical Chemistry B* **1999**, *103*, 10017-10021.

(30) Mao, Y.; Ratner, M. A.; Jarrold, M. F. *Journal of the American Chemical Society* **2001**, *123*, 6503-6507.

(31) Mao, Y.; Woenckhaus, J.; Kolafa, J.; Ratner, M. A.; Jarrold, M. F. *Journal of the American Chemical Society* **1999**, *121*, 2712-2721.

(32) Jarrold, M. F. *Accounts of Chemical Research* **1999**, *32*, 360-367.

(33) Woenckhaus, J.; Mao, Y.; Jarrold, M. F. *Journal of Physical Chemistry B* **1997**, *101*, 847-851.

(34) Hoaglund-Hyzer, C. S.; Counterman, A. E.; Clemmer, D. E. *Chemical Reviews* **1999**, *99*, 3037-3079.

(35) Jarrold, M. F. *Annual Review of Physical Chemistry* **2000**, *51*, 179-207.

(36) Baker, E. S.; Bernstein, S. L.; Gabelica, V.; De Pauw, E.; Bowers, M. T. *International Journal of Mass Spectrometry* **2006**, *253*, 225-237.

(37) Rueda, M.; Kalko, S. G.; Luque, F. J.; Orozco, M. *Journal of the American Chemical Society* **2003**, *125*, 8007-8014.

(38) Rueda, M.; Luque, F. J.; Orozco, M. *Journal of the American Chemical Society* **2005**, *127*, 11690-11698.

(39) Arteca, G. A.; Reimann, C. T.; Tapia, O. *Mass Spectrometry Reviews* **2001**, *20*, 402-422.

(40) Nemethy, G.; Steinberg, I. Z.; Scheraga, A. *Biopolymers* **1963**, *1*, 43-69.

(41) Steinbach, P. J.; Brooks, B. R. *Proceedings of the National Academy of Sciences of the United States of America* **1993**, *90*, 9135-9139.

(42) Steinbach, P. J.; Hodoscek, M.; Brooks, B. R. *Biophysical Journal* **1993**, *64*, A183-a183.

(43) Smith, J. C.; Merzel, F. *Abstracts of Papers of the American Chemical Society* **2002**, *224*, U316-U316.

(44) Smith, J. C.; Merzel, F.; Bondar, A. N.; Tournier, A.; Fischer, S. *Philosophical Transactions of the Royal Society of London Series B-Biological Sciences* **2004**, *359*, 1181-1189.

(45) Smith, J. C.; Merzel, F.; Verma, C. S.; Fischer, S. *Journal of Molecular Liquids* **2002**, *101*, 27-33.

(46) Niccolai, N.; Spiga, O.; Bernini, A.; Scarselli, M.; Ciutti, A.; Fiaschi, I.; Chiellini, S.; Molinari, H.; Temussi, P. A. *Journal of Molecular Biology* **2003**, *332*, 437-447.

(47) Pevsner, A.; Diem, M. *Biopolymers* **2003**, *72*, 282-289.

(48) Lubarsky, G. V.; Davidson, M. R.; Bradley, R. H. *Biosensors & Bioelectronics* **2007**, *22*, 1275-1281.

(49) Liu, Y.; Fratini, E.; Baglioni, P.; Chen, W. R.; Chen, S. H. *Physical Review Letters* **2005**, *95*, -.

(50) Winger, B. E.; Lightwahl, K. J.; Smith, R. D. *Journal of the American Society for Mass Spectrometry* **1992**, *3*, 624-630.

(51) Elber, R.; Roitberg, A.; Simmerling, C.; Goldstein, R.; Li, H. Y.; Verkhivker, G.; Keasar, C.; Zhang, J.; Ulitsky, A. *Computer Physics Communications* **1995**, *91*, 159-189.

(52) Jorgensen, W. L.; Chandrasekhar, J.; Madura, J. D.; Impey, R. W.; Klein, M. L. *Journal of Chemical Physics* **1983**, *79*, 926-935.

(53) Jorgensen, W. L.; Tirado-Rives, J. *Proceedings of the National Academy of Sciences of the United States of America* **2005**, *102*, 6665-6670.

(54) Banci, L.; Bertini, I.; Gray, H. B.; Luchinat, C.; Reddig, T.; Rosato, A.; Turano, P. *Biochemistry* **1997**, *36*, 9867-9877.

(55) Miteva, M. A.; Kossekova, G. P.; Villoutreix, B. O.; Atanasov, B. P. *Journal of Photochemistry and Photobiology B-Biology* **1997**, *37*, 74-83.

(56) Breuker, K. *International Journal of Mass Spectrometry* **2006**, *253*, 249-255.

(57) Ryckaert, J. P.; Ciccotti, G.; Berendsen, H. J. C. *Journal of Computational Physics* **1977**, *23*, 327-341.

(58) Wriggers, W.; Mehler, E.; Pitici, F.; Weinstein, H.; Schulten, K. *Biophysical Journal* **1998**, *74*, 1622-1639.